Molecular dysprosium complexes for white-light and near-infrared emission controlled by the coordination environment

Dimitrije Mara, Flavia Artizzu, Joydeb Goura, Manjari Jayendran, Bojana Bokic, Branko Kolaric, Thierry Verbiest, Rik Van Deun

PII: S0022-2313(21)00762-6

DOI: https://doi.org/10.1016/j.jlumin.2021.118646

Reference: LUMIN 118646

To appear in: *Journal of Luminescence*

Received Date: 23 August 2021

Revised Date: 19 November 2021

Accepted Date: 25 November 2021

Please cite this article as: D. Mara, F. Artizzu, J. Goura, M. Jayendran, B. Bokic, B. Kolaric, T. Verbiest, R. Van Deun, Molecular dysprosium complexes for white-light and near-infrared emission controlled by the coordination environment, *Journal of Luminescence* (2021), doi: https://doi.org/10.1016/j.jlumin.2021.118646.

Author Statement

Dimitrije Mara: Conceptualization, Methodology, Formal Analysis, Investigation, Data Curation, Writing – Original Draft

Flavia Artizzu: Formal Analysis, Validation, Writing – Review & Editing

Joydeb Goura: Validation, Writing – Review & Editing

Manjari Jayerdran: Writing – Review & Editing

Bojana Bokic: Formal Analysis, Writing – Review & Editing

Brako Kolaric: Formal Analysis, Validation, Writing – Review & Editing

Thierry Verbiest: Supervision, Writing – Review & Editing

Rik Van Deun: Supervision, Resources, Writing – Review & Editing

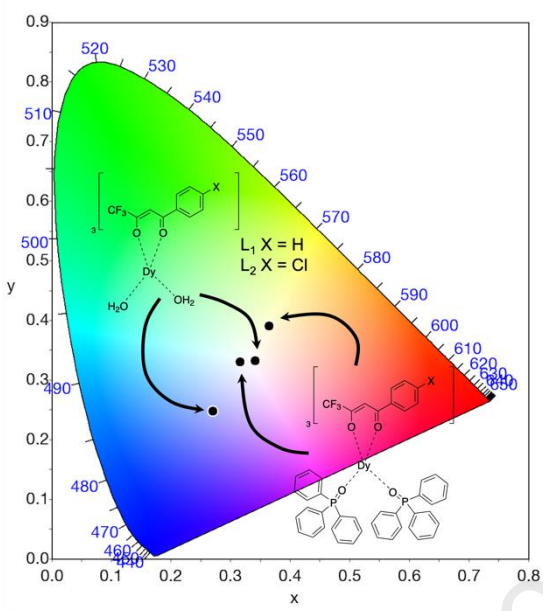

Changes in the coordination environment around the Dy^{3+} ion allow for emission color tunability from blue to white or from cold WLE to warm WLE.

Molecular Dysprosium Complexes for White-Light and Near-Infrared Emission Controlled by the Coordination Environment

Dimitrije Mara[a*], Flavia Artizzu[b,c], Joydeb Goura[b], Manjari Jayendran[b], Bojana Bokic[d], Branko Kolaric[d,e], Thierry Verbiest[a], Rik Van Deun[b*]

[a] – Molecular Imaging and Photonics, Department of Chemistry, KU Leuven, Celestijnenlaan 200 D, box 2425, B-3001, Leuven, Belgium.
[b] – L^3 – Luminescent Lanthanide Lab, Department of Chemistry, Ghent University, Krijgslaan 281 – S3, B-9000, Ghent, Belgium.
[c] – Department of Sciences and Technological Innovation, University of Eastern Piedmont "Amedeo Avogadro", Viale Teresa Michel 11, 15112 Alessandria, Italy.
[d] – Photonics Center, Institute of Physics, University of Belgrade, Pregrevica 118, 11080, Belgrade, Serbia.
[e] – Micro- and Nano-photonics Materials Group, University of Mons, Avenue Maistriau 19, B-7000, Mons, Belgium.

[*] Corresponding authors: dimitrije.mara@kuleuven.be (D. Mara), rik.vandeun@ugent.be (R. Van Deun)

Abstract

A series of single-molecule dysprosium (Dy^{3+}) complexes consisting of β-diketonate ligands, L_1 = 4,4,4-trifluoro-1-phenyl-1,3-butadionate and L_2 = 4,4,4-trifluoro-1-(4-chlorophenyl)-1,3-butadionate, as water-containing complexes, and the auxiliary triphenylphosphine oxide (tppo) ligand as water-free complexes were investigated as potential white-light emitters. The coordination environment and choice of the ligands play an important role in the behavior of the yellow/blue emission of the Dy^{3+} complexes (Y: $^4F_{9/2} \rightarrow {}^6H_{13/2}$ – yellow, and B: $^4F_{9/2} \rightarrow {}^6H_{15/2}$ and ligand phosphorescence – blue) based on the sensitization efficiency of the Dy^{3+} ion by the ligands. By introducing the auxiliary tppo ligand in the complex, the relative intensity of the Dy^{3+} emission increases due to a more efficient sensitization of the Dy^{3+} ion. The CIE (Commission International d'Eclairage) coordination at room temperature for water-containing, **DyL_1H_2O** (0.340, 0.333), and **DyL_2H_2O** (0.270, 0.249), and for water-free complexes, **DyL_1tppo** (0.364,0.391) and **DyL_2tppo** (0.316, 0.331), are close to the coordinates of 'ideal' white light (0.333, 0.333). The CCT (Correlated Color Temperature) values at room temperature for **DyL_1H_2O** (5129 K), **DyL_2H_2O** (18173 K), and **DyL_2tppo** (6319 K) correspond to 'cold-white-light' emitters, while the **DyL_1tppo** (4537 K) matches a 'warm-white-light' emitter. Beside emitting in the visible (Vis) region, the Dy^{3+} complexes also show emission in the near-infrared (NIR) part of spectrum, which has been studied in detail.

Keywords: White-light emission, Lanthanide complexes, Luminescence, NIR emission

1. Introduction

The growth of the global energy consumption has accelerated development and usage of energy-saving smart devices and energy-efficient solid-state lighting (SSL). Solid-state white-light-emitting materials posses exceptional properties such as energy saving and long operational lifetime, which has already led to their widespread application covering large-panel displays to ambient lighting. [1-3] First, the SSL sources can be subdivided based on the materials, from which they are made of, either inorganic phosphors (LED) or organic molecule semiconductors (OLDE). From another perspective, the SSLs are subdivided in two categories based on the way they are stimulated to emit light, that is, by UV excitation (LEDs) or by electrical excitation (OLEDs). SSLs are much more efficient compared to the classical incandescent lamps, or environmentally friendly as compared to fluorescent and mercury lamps. [4-6]

In general, there are two different approaches to obtain white-light emission (WLE): using dichromatic emitters (blue and yellow (B/Y) or blue and red (B/R)), or by using trichromatic emitters which combine the three primary colors (red, green, and blue (RGB)). [1,7-19] White light is obtained by using separate dopants or multiple phase matrices such as organic compounds, metal complexes, nanomaterials, hybrid organic-inorganic materials or inorganic phosphors. All these types of materials have some unique characteristics to exploit their advantages in obtaining white light, but sometimes it is necessary to mix different types of materials to achieve the intended goal. On the other hand, white-light emission (WLE) from single molecules can also be achieved, spanning the whole visible (Vis) spectrum. [20-25] The advantage of such systems is that they consist of a single phase single emitter, and this simplifies the production of lighter and thinner materials, which is highly favorable for the implementation of optical devices. [26]

Additionally, because of the unique properties of the lanthanide (Ln^{3+}) ions, lanthanide complexes, are interesting platforms for applications in lighting technologies. The Ln^{3+} luminescence arises from 4f – 4f transitions, which correspond to characteristic colors (wavelengths) from the ultra-violet (UV) across the Vis to the near-infrared (NIR) spectral region. Unfortunately, the 4f – 4f transitions are difficult to excite directly according to Laporte's rule and a way to overcome this disadvantage is by using organic chromophores which act as antenna to sensitize the Ln^{3+} ions. [27] β-Diketonate complexes are well known in lanthanide coordination chemistry and have been studied in extent. [28,29] Their ability to

excite virtually every spectroscopically active Ln^{3+} ion to obtain the pure Ln^{3+} luminescence colors, as well as their processability into more complex matrices creates the opportunity for a wide range of applications, such as lighting, ion sensing, temperature sensing, telecommunications, etc. [30-33] The organic chromophores in this case should be designed or chosen to act as antennas for the Ln^{3+}, but at the same time they should be able to emit by themselves to yield the blue component necessary to obtain white light. The design of such WLE Ln^{3+} complexes is in fact typically based on the combination of an organic chromophore which emits in the blue region, with a Ln^{3+} ion that emits in the yellow (Dy^{3+}) or in the red (Eu^{3+}) region. [34-50]

Here, we present a series of single-molecule WLE tris Dy^{3+} β-diketonate complexes of two different β-diketonate ligands (4,4,4-trifluoro-1-phenyl-1,3-butadionate and 4,4,4-trifluoro-1-(4-chlorophenyl)-1,3-butadionate), with either coordinated water molecules or triphenylphosphine oxide (tppo) as co-ligand, which can be excited at 365 nm. [50,51] Simultaneous emission from the ligand and Dy^{3+} has been observed, giving rise to WLE, which by modifying the coordination environment, could be altered from deep cold (blue) to warm (yellow) white light. In addition to white emission in the Vis region, the series of Dy^{3+} complexes also showed emission in the NIR spectral region.

2. **Experimental Section**

2.1. Materials

$DyCl_3 \cdot 6H_2O$ (99.9%), 4,4,4-trifluoro-1-phenyl-1,3-butadione (Hbfa) 99% and triphenylphosphine oxide 98% were purchased from Sigma Aldrich. The 4,4,4-trifluoro-1-(4-chlorophenyl)-1,3-butadione 98% was purchased from TCI Europe. Methanol (laboratory grade, 100%) and NaOH were purchased from Fisher Scientific. All chemicals were used without further purification. All reaction were carried out under atmospheric conditions.

2.2. Synthesis of $[Dy(L_{1(2)})_3(H_2O)_2]$ and $[Dy(L_{1(2)})_3(tppo)_2]$ complexes

The synthesis procedure has been previously reported in detailed and will be only discussed in short. [51] The synthesis of $[Dy(L_{1(2)})_3(H_2O)_2]$ was done in methanol by first dissolving an appropriate amount of ligand L_1 and L_2 (0.9 mmol), which were then deprotonated with an equimolar amount of NaOH prior to the addition of methanol solution of $DyCl_3 \cdot 6H_2O$ (0.3 mmol). The obtained crystals were recrystallized from methanol solution and used for further analysis. The synthesis of $[Dy(L_{1(2)})_3(tppo)_2]$ was done in methanol, by addition of a methanol solution of $[Dy(L_{1(2)})_3(H_2O)_2]$ (0.1 mmol) to dissolve triphenylphosphine oxide (tppo) (0.2 mmol) and the complexes were used without any additional purification. No crystals suitable

for single crystal X-ray diffraction could be obtained due to the formation of twinned crystals during crystallization.

$[Dy(L_1)_3(H_2O)_2]$ **DyL_1H_2O**: Elemental analysis (%) calculated for $C_{30}H_{22}F_9O_8Dy$ (847.00): C 42.54, H 2.98, found: C 42.45, H 2.93. FT-IR (KBr) ν_{max} (cm^{-1}):): 3657 (s; νst O-H, free), 3449 (w; νst O-H, H-bonded), 3083, 2774, 2601, 2525 (w; νst C-H and Fermi resonance), 2482, 2381, 2321, 2273, 2229, 2137 (w; aromatic overtone), 2085 2044, 1985, 1908, 1863, 1820, 1775 (w; comb, aromatic), 1667 (w; νst C=O, keto form), 1628, 1571, 1532, 1493, 1467 (w; νst ar C-C), 1379, 1288 (w; νst C-F, CF3), 1249, 1197, 1144 (w; νst C-F, CF3 and δip ar C-H), 1096 (w), 1027 (s; δip ar C-H), 996 (s; δoop C-H), 817 (w; γ ar C-C and νst C-Cl), 773, 721 (w; δ C-F, CF3, δoop C-H and γ ar C-C and νst C-Cl). ESI-MS (negative mod, -), m/z: 868.00 $[M+Na-2H]^-$, 1023.97 $[M+2Br+H]^-$ Isotope used for calculation is ^{164}Dy.

$[Dy(L_2)_3(H_2O)_2]$ **DyL_2H_2O**: Elemental analysis (%) calculated for $C_{30}H_{19}Cl_3F_9O_8Dy$ (950.33): C 37.92, H 2.33; found: C 37.88, H 2.25. FT-IR (KBr) ν_{max} (cm^{-1}): 3657 (s; ν_{st} O-H, free), 3434 (s; ν_{st} O-H, H-bonded), 3072, 2779, 2677, 2591 (w; ν_{st} C-H and Fermi resonance), 2508, 2434, 2389, 2327, 2286, 2232, 2133 (w; aromatic overtone), 2096, 2051, 1911, 1796 (w; comb, aromatic), 1681 (w; ν_{st} C=O, keto form), 1627, 1574, 1536, 1487, 1463 (w; ν_{st} ar C-C), 1401, 1359, 1294 (w; ν_{st} C-F, CF_3), 1248, 1191, 1146 (w; ν_{st} C-F, CF_3 and δ_{ip} ar C-H), 1096 (w), 1014 (s; δ_{ip} ar C-H), 944 (s; δ_{oop} C-H), 849 (w; γ ar C-C and ν_{st} C-Cl), 799, 738, 705, 664 (w; δ C-F, CF_3, δ_{oop} C-H and γ ar C-C and ν_{st} C-Cl). ESI-MS (negative mod, -), m/z: 972.00 $[M+Na-2H]^-$, 1159.00 $[M+2Br+H]^-$. Isotope used for calculation is ^{164}Dy.

$[Dy(L_1)_3(tppo)_2]$ **DyL_1tppo**: Elemental analysis (%) calculated for $C_{66}H_{48}F_9O_8P_2Dy$ (1367.54): C 57.97, H 3.76; found: C 57.88, H 3.70. FT-IR (KBr) ν_{max} (cm^{-1}): 3267, 3147 (w; νst C-O, enol beyond the range), 3061 (s; νst ar C-H), 2965, 2913, 2771, 2710, 2599 (w; νst C-H and Fermi resonance), 2520, 2471, 2434, 2381, 2323, 2278, 2129 (w; aromatic overtone), 2088, 2030, 1969, 1895, 1820 (w; comb, aromatic), 1776, 1713 (w; νst C=O, keto form), 1656, 1577, 1535, 1491, 1442 (w; νst ar C-C), 1376, 1323 (w; νst C-F, CF3), 1290 (w; νst P=O), 1244, 1199, 1146 (w; νst C-F, CF3, δip ar C-H and νst R3P=O), 1094, 1075, 1026 (s; δip ar C-H and νst R3P=O), 997, 972 (w; νst R3P=O), 943 (s; δoop C-H and νst R3P=O), 848, 807, 795 (w; γ ar C-C and νst P-C), 758, 725, 635 (w; δ C-F, CF3, δoop C-H and γ ar C-C). ESI-MS (positive mode +), m/z: 1428.00 $[M+Na+ACN]^+$, 1150.00 $[M-tppo+Na+ACN]^+$, 870.00 $[M-2tppo+Na]^+$. Isotope used for calculation is ^{164}Dy.

$[Dy(L_2)_3(tppo)_2]$ **DyL_2tppo**: Elemental analysis (%) calculated for $C_{66}H_{45}Cl_3F_9O_8P_2Dy$ (1470.87): C 53.89, H 3.29; found: C 53.80, H 3.25. FT-IR (KBr) ν_{max} (cm^{-1}): 3265, 3146 (w; νst C-O, enol beyond the range), 3060 (s; νst ar C-H), 2961, 2920, 2829, 2768, 2714, 2586 (w; νst C-H and Fermi resonance), 2467, 2380, 2327, 2286, 2249, 2129 (w; aromatic overtone), 2088, 2039, 1964, 1898, 1820 (w; comb, aromatic), 1776 (w; νst C=O, keto form), 1627, 1594, 1533, 1483, 1438 (w; νst ar C-C), 1380, 1318 (w; νst C-F, CF3), 1288 (w; νst P=O), 1240, 1187, 1141 (w; νst C-F, CF3, δip ar C-H and νst R3P=O), 1088, 1067, 1030 (s; δip ar C-H and νst R3P=O), 1014, 972 (w; νst R3P=O), 930 (s; δoop C-H and νst R3P=O), 849, 783 (w; γ ar C-C and νst P-C), 725, 693, 660 (w; δ C-F, CF3, δoop C-H and γ ar C-C). ESI-MS (positive mode +), m/z: 1497.87 $[M+Na+ACN]^+$, 1218.87 $[M-tppo+Na+ACN]^+$, 980.00 $[M-2tppo+Na]^+$. Isotope used for calculation is ^{164}Dy.

2.3. Characterization

Luminescence measurements were performed on an Edinburgh Instruments FLSP920 UV-Vis-NIR spectrometer setup. A 450 W Xe lamp was used as steady-state excitation source. Time-resolved measurements were recorded using a 60 W Xe lamp operating at frequency of 100 Hz. A Hamamatsu R928P photomultiplier tube was used to detect emission signal in the visible region. A Hamamatsu R5509-72 multiplier tube was used to detect emission in the NIR region. The absolute quantum yield (QY) of the complex was determined using an integrating sphere coated with BENFLEC (provided by Edinburgh Instruments) and calculated using **Equation 1**:

$$\eta = \frac{\int L_{emission} d\lambda}{\int E_{blank} d\lambda - \int E_{sample} d\lambda} \quad (1)$$

Where $L_{emission}$ is the integrated area under the emission spectrum ($d\lambda$ = 400-700 nm), E_{blank} is the integrated area under the "excitation" band of the blank, and E_{sample} is the integrated area under the excitation band of the sample (as the samples absorbs part of the light, this area will be smaller than E_{blank}). All luminescent measurements were recorded at room temperature. Crystals were put between quartz plates (Starna cuvettes for powder samples, type 20/C/Q/0.2). The time-resolved data were fitted with a biexponential function where the short component (in the range from 1.4 to 1.9 μs) is attributed to the Xe lamp signal, while the longer component is associated to the emission signal of the Dy^{3+} complexes and are presented in Tables 1 and 2. Only for the samples DyL_1tppo and DyL_2tppo the emission signal at ~ 995 nm, with a significantly longer decay time, was fitted with a monoexponential function.

Fourier Transform Infrared (FTIR) spectra were acquired in the region of 400-4000 cm^{-1} with a Thermo Scientific Nicolet 6700 FT-IR spectrometer equipped with a nitrogen-cooled Mercury Cadmium Telluride (MCT) detector and KBr beam splitter; samples were measured in KBr pellets. Elemental analysis (C, H, N) was performed on a Thermo Fisher 2000 elemental analyzer, using V_2O_5 as catalyst. ESI-MS was performed on an Agilent 6230 time-of-flight mass spectrometer (TOF-MS) equipped with Jetstream ESI source and positive and negative ionization modes were used.

3. Results and discussion

3.1. Synthesis and characterization of Dy^{3+} complexes

The complexes were synthesized using mild reaction conditions, where the β-diketonate ligand was deprotonated with an equimolar amount of sodium hydroxide and reacted with the Dy^{3+} ion in a stoichiometric ratio in methanol. The high reactivity of the β-diketonate ligand toward coordination to Dy^{3+} ions prevents the formation of highly insoluble lanthanide hydroxides, which could be formed under basic conditions. The complexes with formula $[Dy(L_1)_3(H_2O)_2]$ (L_1 = 4,4,4-trifluoro-1-phenyl-1,3-butadionate) and $[Dy(L_2)_3(H_2O)_2]$ (L_2 = 4,4,4-trifluoro-1-(4-chlorophenyl)-1,3-butadionate) were isolated. The synthesis of water-free complexes was performed by introducing tppo in methanol solution in a stochiometric ratio to the $[Dy(L_{1(2)})_3(H_2O)_2]$ complex to form and isolate the water-free complexes with formula $[Dy(L_1)_3(tppo)_2]$ and $[Dy(L_2)_3(tppo)_2]$. These complexes have been characterized by FT-IR, ESI-MS (see SI Figs. S1-S8) and elemental analysis which confirmed that all the complexes have the same composition as the previosly reported analogs. [51,52]

3.2. Steady-state and time-resolved photoluminescence (PL) studies

3.2.1. Steady-state and time-resolved PL of Dy^{3+} complexes in the visible region

Upon excitation into the β-diketonate ligand absorption band (see SI Figs. S9-S12) with UV light all studied Dy^{3+} complexes showed emission in the Vis and NIR spectral range displaying the characteristic Dy^{3+} peaks. In Fig. 1, the PL emission spectra of **DyL_1H_2O**, **DyL_1tppo** (a), **DyL_2H_2O** and **DyL_2tppo** (c) are presented. The Dy^{3+} $^4F_{9/2} \rightarrow {}^6H_{15/2}$ transition appearing at 480 nm, the $^4F_{9/2} \rightarrow {}^6H_{13/2}$ transition at 575 nm and the $^4F_{9/2} \rightarrow {}^6H_{11/2}$ transition at 660 nm are clearly observed. Besides the emission peaks of the Dy^{3+} ion, a broad band (400 to 450 nm) with a peak maximum at ~ 430 nm is observed, which is assigned to ligand-centered emission. In water-free complexes the relative intensity of this broad band is lower as compared to its intensity in water-containing complexes. The advantage of the introduction of the tppo ligand into the water-containing complexes brings two benefits:

first, the exclusion of water molecules from the first coordination sphere around the Dy^{3+} ion (reducing quenching) and second, a more efficient energy transfer from the tppo ligand to Dy^{3+}, increasing the relative intensity of the metal peaks in the emission spectra in comparison to the ligand band (Fig. 1. a and c)

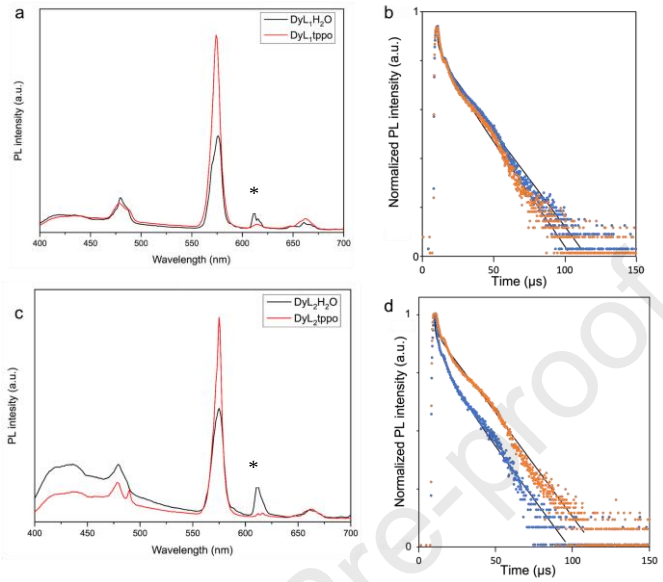

Fig. 1. (a) PL emission spectra of DyL_1H_2O and DyL_1tppo, excited at 365 nm and measured at RT; (b) decay profile of DyL_1H_2O (blue) and DyL_1tppo (orange) observed at 575 nm; (c) PL emission spectra of DyL_2H_2O and DyL_2tppo, excited at 365 nm and measured at RT; (d) decay profile of DyL_2H_2O (blue) and DyL_2tppo (orange) observed at 575 nm. * Contamination of the $DyCl_3{\cdot}6H_2O$ salt with europium salts not influencing the photophysics of Dy^{3+}.

Time-resolved measurements (Figure 1 and Table 1) show that the decay dynamics of the Dy^{3+} $^4F_{9/2}$ level is monoexponential and that the water-free complexes have slightly longer luminescent lifetimes compared to the water-containing complexes, likely because of the reduced quenching efficiency by high-energy oscillators related to the water molecules in the first coordination sphere. The sensitization efficiency of the Dy^{3+} ion in the water-free complexes is estimated to be slightly higher as well, because of the possible contribution of the tppo co-ligand to the process. In fact, to realize an efficient energy transfer (ET), the difference between the energy donor, being the triplet state (T_1) of the ligand, and the acceptor, being the emitting level of the Ln^{3+} ion, should be ideally between 2500 and 3500 cm^{-1}. While an energy match between the donor and acceptor states is key to an efficient ET, a small energy gap, which could easily be overcome in molecular complexes by a vibrationally assisted ET, is also desirable to prevent collateral back energy transfer (BET)

which could reduce the efficiency of the metal-to-ligand sensitization process. [55] This issue is particularly relevant in Dy^{3+} compounds where the long-lived main emitting $^4F_{9/2}$ level is placed at ~21000 cm^{-1}, an energy that is relatively high with respect to the triplet energy level of most organic ligands. In the water-free compounds, the tppo co-ligand has a higher triplet state (T_1 = 23800 cm^{-1}) compared to the triplet states of ligands L_1 (T_1 = 22500 cm^{-1}) and L_2 (T_1 = 21500 cm^{-1}) and is expected to be a more effective antenna towards Dy^{3+}. [54] These observations explain the increased relative intensity of the ligand-centered emission in the derivatives with ligand L_2, particularly with coordinated water, indicating a less effective ligand-to metal sensitization (Figure 1).

Table 1. Luminescence lifetimes and absolute quantum yields in the visible range for the Dy^{3+} complexes.

Compound	τ (μs)	R^2	QY [%]
DyL_1H_2O	9.85	0.996	4.94
DyL_1tppo	11.41	0.996	5.32
DyL_2H_2O	9.38	0.995	3.00
DyL_2tppo	10.49	0.996	3.58

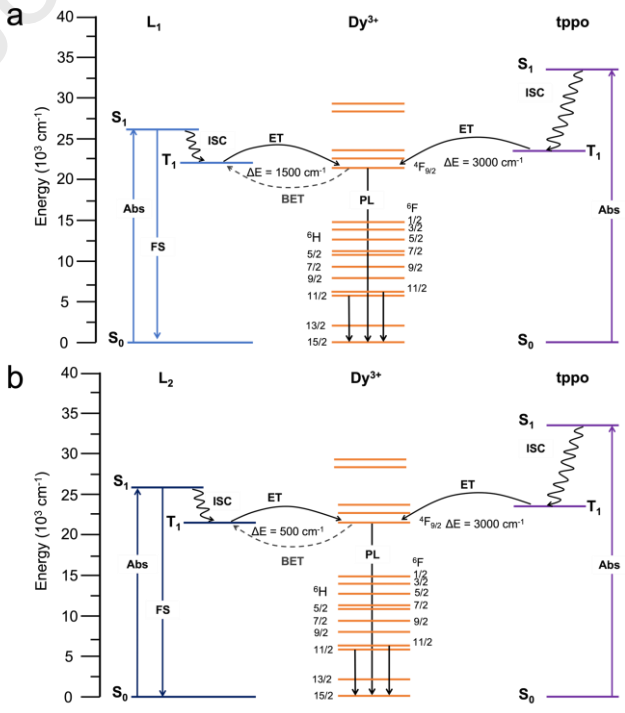

Fig. 2. Jablonski diagram for the Dy^{3+} complexes with the ligand L_1 (a) and with the ligand L_2 (b). S_0 – singlet ground state, S_1 – singlet excited state, T_1 – triplet state, ISC – inter system crossing, ET – energy transfer, BET – back energy transfer, Abs – absorbance, FS – fluorescence, PL – photoluminescence.

3.2.2. Steady-state and time-resolved PL of Dy^{3+} complexes in the NIR region

When exciting into the absorption bands of the ligands, the investigated complexes, **DyL_1H_2O** and **DyL_1tppo** (Fig. 3a and 3b), **DyL_2H_2O** and **DyL_2tppo** (Fig. S13a and 13b in SI), show NIR luminescence. The PL spectrum in the range 800-1650 nm is dominated by the characteristic emission peaks of Dy^{3+} corresponding to the following transitions: $^4F_{9/2} \rightarrow {}^6H_{7/2} + {}^6F_{9/2}$ (846 nm), $^6H_{5/2} + {}^6F_{7/2} \rightarrow {}^6H_{15/2}$ (~994 nm), $^6F_{3/2} \rightarrow {}^6H_{13/2}$ (1066 nm), $^4F_{9/2} \rightarrow {}^6F_{5/2}$ (~1170 nm), $^6F_{11/2} \rightarrow {}^6H_{15/2}$ and $^6H_{9/2} \rightarrow {}^6H_{15/2}$ (~1320 nm), $^4F_{9/2} \rightarrow {}^6F_{1/2}$ (1404 nm) and $^6F_{5/2} \rightarrow {}^6H_{11/2}$ (~1500 nm). [56] However, the **DyL_2H_2O** complex (Fig. S13a) only shows a clear emission peak at 1317 nm while the other peaks in this region are not visible. This is likely ascribable to a significant quenching effect on the Ln^{3+} ion to NIR-emission by high-strength oscillators such as C-H (ν C-H at 1650 nm and 3ν C-H 1130 nm) and O-H (2ν O-H at 1400 nm), especially for water molecules directly bonded to the emitter. [50]

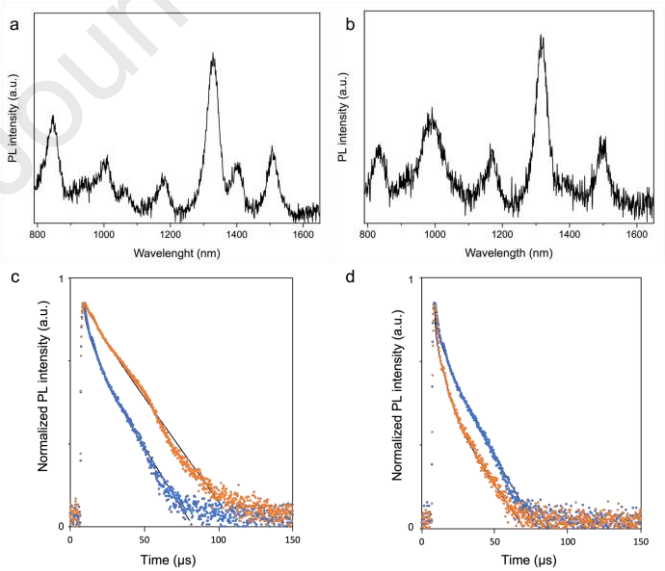

Fig. 3. NIR PL emission spectra of DyL_1H_2O (a) and DyL_1tppo (b), excited at 365 nm and measured at RT; (c) decay profile of DyL_1H_2O (blue) observed at 846 nm, DyL_1tppo (orange) observed at 994 nm; (d) decay profile of DyL_1H_2O (blue) and DyL_1tppo (orange) observed at 1320 nm.

The luminescence decay traces of the Dy^{3+} complexes in the NIR have been recorded at 994 nm and ~1320 nm corresponding to the $^6H_{5/2}$+$^6F_{7/2}$ and $^6H_{9/2}$ + $^6F_{11/2}$ levels, respectively. All decay traces are well fitted with a monoexponential function (see Experimental Section for details), pointing to the existence of one population of emitters and confirming the purity of the samples.

As expectable, for both series of complexes with ligands L_1 and L_2, the emission signal can be only barely detected in water-containing complexes (Figs. 3c and S13c). This effect can be attributed to vibrational quenching through the third harmonic of the OH stretching, as was previously observed in analogous Yb^{3+} complexes. [51] Interestingly, the decay dynamics of the $^6F_{11/2}$ + $^6H_{9/2} \rightarrow {}^6H_{15/2}$ transition at 1320 nm is very similar for the water-containing complexes and the tppo derivates of the same ligands. This finding seems apparently in contrast with the expected shortening of the lifetimes in the presence of bound water molecules and with observation made for the relaxation of the $^4F_{9/2}$ level. However, the change of the coordination environment, following the replacement of water molecules by tppo ligands, is likely to induce a significant variation of the oscillator strength of the transition, possibly leading to a decrease of the radiative lifetime in the water-free compounds. [51, 57] This could therefore explain the similar observed lifetimes despite the envisaged quenching effect by water molecules. It should be also noted that the discrepancy of the observed lifetime values between the complexes with ligands L_1 and L_2 (Table 2), despite the similar amount of quenching sites, is attributed to a difference in the radiative lifetime dynamics induced by the subtle differences in the ligand structure, further highlighting the relevant role of the coordination environment of the emission properties of these compounds.

Table 2. Observed luminescence decay time constants and corresponding Dy^{3+} transitions.

Compound	λ (nm)	Transition	τ (μs)	R^2
DyL_1H_2O	846	$^4F_{9/2} \rightarrow {}^6H_{7/2}$ + $^6F_{9/2}$	10.82	0.998
	1320	$^6F_{11/2} \rightarrow {}^6H_{15/2}$ $^6H_{9/2} \rightarrow {}^6H_{15/2}$	10.34	0.997
DyL_1tppo	994	$^6F_{7/2} \rightarrow {}^6H_{15/2}$ $^6H_{5/2} \rightarrow {}^6H_{15/2}$	15.07	0.997
	1320	$^6F_{11/2} \rightarrow {}^6H_{15/2}$ $^6H_{9/2} \rightarrow {}^6H_{15/2}$	10.71	0.998
DyL_2H_2O	1320	$^6F_{11/2} \rightarrow {}^6H_{15/2}$ $^6H_{9/2} \rightarrow {}^6H_{15/2}$	10.73	0.996
DyL_2tppo	994	$^4F_{9/2} \rightarrow {}^6F_{7/2}$	16.33	0.998
	1320	$^6F_{11/2} \rightarrow {}^6H_{15/2}$ $^6H_{9/2} \rightarrow {}^6H_{15/2}$	10.34	0.997

3.3. White-light emission (WLE) of Dy^{3+} complexes

The CIE chromaticity diagram (Fig. 4) shows that the Dy^{3+} complexes with both ligands, L_1 and L_2, are emitting in the region from cold to warm white light upon excitation with UV light (365 nm). Exciting by different wavelengths in the ligand absorption bands did not result in significant emission differences. According to the CIE coordinates (Table 3) obtained for the **DyL_1H_2O** and **DyL_2tppo** complexes, the emitted white light is close to the pure white light (CIE 1931 chromaticity x = 0.333, y = 0.333) with Correlated Color Temperatures (CCT) of 5470 K. Instead, the CIE coordinates for the **DyL_1tppo** complex are more situated toward the warm white light region leaning toward yellow-white light and the **DyL_2H_2O** complex shows emission in the cold-white light region, corresponding to blueish-white light. As it can be seen in the CIE diagram, color tunability was achieved by changing the coordination environment by introducing the auxiliary tppo ligand. This resulted in tuning the color for the complexes with ligand L_2 from blue to white light, while for the complexes with ligand L_1 the color was tuned from white to yellow-white light. The observed tunability is in accordance with the decrease of the intensity of the residual blue emission from the β-diketonate ligand upon introduction of the tppo co-ligand, as previously discussed.

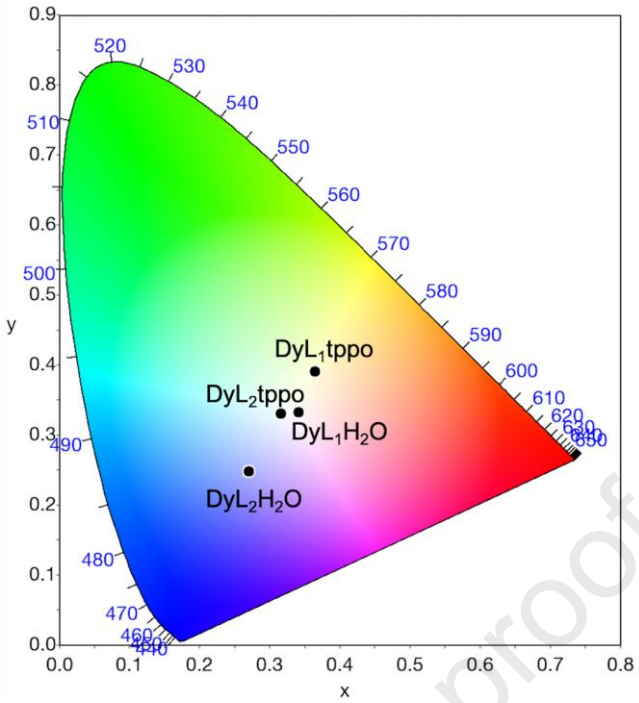

Fig. 4. The CIE chromaticity diagram with the color coordinates of the Dy^{3+} complexes excited at 365 nm.

Table 3. CIE color coordinates (x,y) and CCT for the Dy^{3+} complexes in the solid state.

Compound	x	y	CCT (K)
DyL_1H_2O	0.340	0.333	5129
DyL_1tppo	0.364	0.391	4537
DyL_2H_2O	0.270	0.249	18173
DyL_2tppo	0.316	0.331	6319

4. Conclusions

A series of water-containing and water-free Dy^{3+} β-diketonate complexes were prepared with two ligands, L_1 and L_2, with similar chemical properties but with a slight structural difference. In the ligand L_2 the H-atom of the phenyl ring in *para*-position to the β-diketonate group was substituted with a Cl-atom. The water-free complexes have been prepared with a neutral tppo co-ligand that excludes water molecules from the first coordination sphere of the Dy^{3+} ion and acts as an additional sensitizer for energy transfer to the nearby Dy^{3+} ion. All the complexes showed emission with characteristic transitions in both Vis and NIR region. The proximity of the energies of the triplet (T_1) states of ligands L_1 and L_2 to the emitting level of Dy^{3+} ($^4F_{9/2}$) led to a partial depopulation of the ligand excites states and resulted in the observation of ligand

emission in the visible blue in addition to the emission of the Dy^{3+} ion in the yellow-green region. This was exploited to obtain white-light emission. The observed WLE of **DyL_1H_2O** (x = 0.340, y = 0.333) and **DyL_2tppo** (0.316, 0.331) is close to ideal white light with CCT in the cold white-light region. Interestingly, the complexes also yield the rarely observed Dy^{3+} -centered NIR emission with a peak at 1320 nm falling in the O-band region of interest in optical telecommunications. The careful design of a ligand that would promote the emission in the NIR region, without enhancing the quenching of Dy^{3+} emission in this region, could introduce Dy^{3+} as an alternative to the commonly used NIR-emitting lanthanide ions, such as Er^{3+} and Nd^{3+}, that are currently exploited for optical telecommunications. Also the possibility of wider use such as multifunctional molecular materials such as optical applications (lighting) and molecular magnets can be interesting for further design.

Conflict of interest

There are no conflicts to declare.

Acknowledgment

DM and TV acknowledge KU Leuven Postdoctoral Mandate Internal Funds (PDM) for a postdoctoral fellowship (PDM/20/092). BK and BB acknowledge financial support of The Ministry of Education, Science and Technological Development of The Republic of Serbia. BK also acknowledge support from F R S-FNRS.

Supporting Information

In the Supporting Information are the additional PL spectra, FT-IR and ESI-MS data.

Reference

[1] E. F. Schobert, J. K. Kim, Sciences 308 (2005) 1274-1278.
[2] C. Feldmann, T. Jüstel, C. R. Ronda, P. J. Schmidt, Adv. Funct. Mater. 13 (2003) 511-516.
[3] T. Jüstel, H. Nikol, C. Ronda, Angew. Chem. Int. Ed. 37 (1998) 3084-3103.
[4] A. De Almeida, B. Santos, B. Paolo, M. Quicheron, Renew. Sustain. Energy Rev. 34 (2014) 30-48.
[5] H. A. Höppe, Angew. Chem. Int. Ed. 48 (2009) 3572-3582.
[6] N. T. Kalyani, S. J. Dhoble, Renew. Sustain. Energy Rev. 16 (2016) 2696-2723.
[7] J. Leng, H. Li, P. Chen, W. Sun, T. Gao, P. Yan, Dalton Trnas. 43 (2014) 12228-12235.
[8] E. Ravindra, S. J. Anathakrisahnan, E. Varanthan, V. Subramanian, N. Somanathan, J. Mater. Chem. C 3 (2015) 4359-4371.
[9] A. H. Shelton, I. V. Sazanovich, J. A. Weinstein, M. D. Ward, Chem. Commun. 48 (2012) 2749-2751.

[10] S. Kamal, K. P. Bera, M. Usman, B. Sainbileg, S. Mendiratta, A. Pathak, A. I. Inamdar, C.-H. Hung, M. Hayashi, Y.-F. Chen, K.-L. Lu, ACS Appl. Nano Mater. 4 (2021) 2395-2403.
[11] J. Qui, C. Yu, X. Wang, Y. Xie, A. M. Kirillov, W. Huang, J. Li, P. Gao, T. Wu, Q. Nie, D. Wu, Inorg. Chem. 58 (2019) 4524-4533.
[12] T. S. Mahapatra, H. Singh, A. Maity, A. Dey, S. K. Prananik, E. Suresh, A. Das, J. Mater. Chem. C 6 **(**2018) 9756-9766.
[13] Z. Zhang, Y. Chen, H. Chang, Y. Wang, X. Li, X. Zhu, J. Mater. Chem. C 8 (2020) 2205-2210.
[14] Y. Yang, L. Chen, F. Jiang, M. Yu, X. Wan, B. Zhang, M. Hong, *J.* Mater. Chem. C 5 (2017) 1981-1989.
[15] S. Reineke, F. Lindner, G. Schwartz, N. Seidler, K. Walzer, B. Lüssem, K. Leo, Nature 459 (2009) 234-238.
[16] J. Xue, X. Xu, Y. Zhu, D. Yang, J. Mater. Chem. C 8 (2020) 3380-3385.
[17] Q. Zhu, L. Zhang, K. Van Vilet, A. Miserez, N., ACS Appl. Mater. Interfaces 10 (2018) 10409-10418.
[18] L. Xu, Y. Li, Q. Pan, D. Wang, S. Li, G. Wang, Y. Chen, P. Zhu, W. Qin, ACS Appl. Mater. Interfaces 12 (2020) 18934-18943.
[19] M. Zhang, J. Xue, Y. Zhu, C. Yao, D. Yang, ACS Appl. Mater. Interfaces 12 (2020) 22191-22199.
[20] Z. Chen, C.-L. Ho, L. Wang, W. Y. Wong, Adv. Funct. Mater. 32 (2020) 1903269.
[21] Z. Xie, Q. Huang, T. Yu, L. Wang, Z. Mao, W. Li, Z. Yang, Y. Zhang, S. Liu, J. Xu, Z. Chi, M. P. Aldred, Adv. Funct. Mater. 27 (2017) 1703918.
[22] J. Chen, J. Wang, X. Xu, J. Li, J. Song, S. Lan, S. Liu, B. Cai, B. Han, J. T. Precht, D. Ginger, H. Zeng, Nat. Photonics 15 (2021) 238-244.
[23] M. Chen, Y. Zhao, L. Yan, S. Yang, Y. Zhu, I. Murtaza, G. He, H. Meng, W. Huang, Angew. Chem. Int. Ed. 56 (2017) 722-727.
[24] J. Manzur, R. C. De Santana, L. J. Q. Maia, A. Vega, E. Spodine, Inorg. Chem. 58 (2019) 10012-10018.
[25] R. Bouddula, K. Singh, S. Giri, S. Vaidyanathan, Inorg. Chem. 56 (2017) 10127-10130.
[26] G.-L. Law, K.-L. Wong, H.-L. Tam, K.-W. Cheah, W.-T. Wong, Inorg. Chem. 48 (2009) 10492-10494.
[27] S. I. Weissman, J. Chem. Phys. 10 (1942) 214-217.
[28] K. Binnemans, *Handbook on Physics and Chemistry of Rare Earths,* Vol. 35 (Eds.: A. K. Jr. Gschneider, J.-C. G. Bünzli, K. V. Pecharsky), Elsevier B. V., Amsterdam, **2005**, pp. 107-272.
[29] D. J. Bray, J. K. Cleeg, L. F. Lindoy, D. Schilter, Adv. Inorg. Chem. 59 (2006) 1-37.
[30] S. V. Eliseeva, J.-C. G. Bünzli, New. J. Chem. 35 (2011) 1165-1176.
[31] K. Binnemans, Chem. Rev. 109 (2009) 4283-4374.
[32] D. Mara, F. Artizzu, B. Laforce, L. Vincze, K. Van Hecke, R. Van Deun, A. M. Kaczmarek, J. Lumin. 213 (2019) 343-355.
[33] Y. Yang, P. Wang, L. Lu, Y. Fan, C. Sun, L. Fan, C. Xu, A. M. El-Toni, M. Alhoshan, F. Zhang, Anal. Chem. 40 (2018) 7946-7952.
[34] S. V. Eliseeva, E. V. Salerno, B. A. Lopez Bermudez, S. Petoud, V. L. Pecoraro, J. Am. Chem. Soc. 142 (2020) 16173-16176.
[35] R. Devi, K. Singh, S. Vaidyanathan, J. Mater. Chem. C 8 (2020) 8643-8653.
[36] L. Zhong, W.-B. Chen, Z.-J. OuYang, M. Yang, Y.-Q. Zhang, S. Gao, M. Schulze, W. Wernsdofer, W. Dong, Chem. Commun. 56 (2020) 2590-2593.
[37] W. A. Dar, Z. Ahmed, K. Iftikhar, J. Photochem. Photobiol. A. Chem. 356 (2018,) 502-511.

[38] J. Wang, S. Chorazy, K. Nakabayashi, B. Sieklucka, S.-i. Ohkosi, J. Mater. Chem. C 6 (2018) 473-481.
[39] Q.-Y. Yang, K. Wu, J.-J. Jiang, C.-W. Hsu, M. Pan, J.-M. Lehn, C.-Y. Su, Chem. Commun. 50 (2014) 7702-7704.
[40] Z.-F. Li, L. Zhou, J.-B. Yu, H.-J. Zhang, R.-P. Deng, Z.-P. Peng, Z.-Y. Guo J. Phys. Chem. C 111 (2007) 2295-2300.
[41] P.-H. Guo, J.-L. Liu, J.-H. Jia, J. Wang, F.-S. Guo, Y.-C. Chen, W.-Q. Lin, J.-D. Leng, D.-H. Bao, Z.-D. Zhang, J.-H. Luo, M.-L. Tong, Chem. Eur. J. 19 (2013) 8769-8773.
[42] L. Zhong, W.-B. Chem, X.-H. Li, Z.-J. OuYang, M. Yang, Y.-Q. Zhang, S. Gao, W. Dong, Inorg. Chem. 59 (2020) 4414-4423.
[43] J. Chen, Z. Xie, L. Meng, Z. Hu, X. Kuang, Y. Xie, C.-Z. Lu, Inorg. Chem. 59 (2020) 6963-6977.
[44] Z. Wang, H. Yang, P. He, Y. He, J. Zhao, H. Tang, Dalton Trans. 45 (2016) 2839-2844.
[45] Y. Wei, Q. Li, R. Sa, K. Wu, Chem. Commun. 50 (2014) 1820-1823.
[46] Y.-H. Zhang, X. Li, S. Song, Chem. Commun. 49 (2013) 10397-10399.
[47] Y. S. L. V. Narayana, S. Basak, M. Baumgarten, K. Müllen, R. Chandrasekar, Adv. Funct. Mater. 23 (2013) 5875-5880.
[48] D. Sykes, I. S. Tidmarsh, A. Barbieri, I. V. Sanzanovich, J. A. Weinstein, M. D. Ward, Inorg. Chem. 50 (2011) 11323-11339.
[49] P. Coppo, M. Duati, V. N. Kozhevnikov, J. W. Hofstraat, L. De Cola, Angew. Chem. Int. Ed. 44 (2005) 1806-1810.
[50] D. Mara, L. Pilia, M. Van de Steen, I. Miletto, M. Zeng, K. Van Hecke, A. Serpe, P. Deplano, R. Van Deun, F. Artizzu, J. Mater. Chem. C. 9 (2021) 15641-15648.
[51] D. Mara, F. Artizzu, P. F. Smet, A. M. Kaczmarek, K. Van Hecke, R. Van Deun, Chem. Eur. J. 25 (2019) 15944-15956.
[52] D. Mara, A. M. Kaczmarek, F. Artizzu, A. Abalymov, A. G. Skirtach, K. Van Hecke, R. Van Deun, Chem. Eur. J. 27 (2021) 6479-6488.
[53] M. Pietraszkiewicz, O. Pietraszkiewicz, J. Karpiuk, A. Majka, G. Kutkiewicz, T. Borowiak, A. M. Kaczmarek, R. Van Deun, J. Lumin. 170 (2016) 411-419.
[54] A. Zhang, J. Zhang, Q. Pan, S. Wang, H. Jia, B. Xu, J. Lumin. 132 (2012) 965-971.
[55] M. Latva, H. Takalo, V.-M. Mukkala, C. Matachescu, J. C. Rodrígez-Ubis, J. Kankare, J. Lumin. 75 (1997) 149-169.
[56] W. T. Carnall, P. R. Fields, K. Rajnak, J. Chem. Phys. 49 (1968) 4424-4442.
[57] J. Liu, P. Geiregat, L. Pilia, R. Van Deun, F. Artizzu, Adv. Optical Mater. 9 (2021), 2001678.

- Influence of coordination environment on the efficiency of sensitization of Dy^{3+} ion
- White-light emission based on single molecular materials based on Dy^{3+} complexes
- The change of coordination environment on the change of white-light emission color
- Near-infrared emission of Dy^{3+} complexes with intense and long-lived emission at 1320 nm

Conflict of interest

There are no conflicts to declare.